

# UC Berkeley

## UC Berkeley Previously Published Works

### Title

Synergistic Porosity and Charge Effects in a Supramolecular Porphyrin Cage Promote Efficient Photocatalytic CO<sub>2</sub> Reduction\*\*

### Permalink

<https://escholarship.org/uc/item/96f348jw>

### Journal

Angewandte Chemie International Edition, 62(5)

### ISSN

1433-7851

### Authors

An, Lun

De La Torre, Patricia

Smith, Peter T

et al.

### Publication Date

2023-01-26

### DOI

10.1002/anie.202209396

### Copyright Information

This work is made available under the terms of a Creative Commons Attribution-NonCommercial License, available at <https://creativecommons.org/licenses/by-nc/4.0/>

### Peer reviewed



How to cite: Angew. Chem. Int. Ed. 2023, 62, e202209396

International Edition: doi.org/10.1002/anie.202209396

German Edition: doi.org/10.1002/ange.202209396

# Synergistic Porosity and Charge Effects in a Supramolecular Porphyrin Cage Promote Efficient Photocatalytic CO<sub>2</sub> Reduction\*\*

Lun An<sup>+</sup>, Patricia De La Torre<sup>+</sup>, Peter T. Smith, Mina R. Narouz, and Christopher J. Chang\*

**Abstract:** We present a supramolecular approach to catalyzing photochemical CO<sub>2</sub> reduction through second-sphere porosity and charge effects. An iron porphyrin box (**FePB-2(P)**) bearing 24 cationic groups, was made via post-synthetic modification of an alkyne-functionalized supramolecular synthon. **FePB-2(P)** promotes the photochemical CO<sub>2</sub> reduction reaction (CO<sub>2</sub>RR) with 97% selectivity for CO product, achieving turnover numbers (TON) exceeding 7000 and initial turnover frequencies (TOF<sub>max</sub>) reaching 1400 min<sup>-1</sup>. The cooperativity between porosity and charge results in a 41-fold increase in activity relative to the parent Fe tetraphenylporphyrin (**FeTPP**) catalyst, which is far greater than analogs that augment catalysis through porosity (**FePB-3(N)**, 4-fold increase) or charge (Fe *p*-tetramethylanilinium porphyrin (**Fe-p-TMA**), 6-fold increase) alone. This work establishes that synergistic pendants in the secondary coordination sphere can be leveraged as a design element to augment catalysis at primary active sites within confined spaces.

## Introduction

Conversion of carbon dioxide (CO<sub>2</sub>) into value-added chemical feedstocks using renewable energy inputs represents a sustainable solution to simultaneously mitigate growing global energy demands and reduce greenhouse gas concentrations.<sup>[1]</sup> These challenges continue to motivate widespread efforts in the development of new catalyst systems for the electrochemical and photochemical CO<sub>2</sub> reduction reaction (CO<sub>2</sub>RR).<sup>[2]</sup> In this regard, homogeneous

catalysts featuring well-defined metal active sites and ligand scaffolds are valuable in elucidating structure/activity relationships and mechanisms with molecular-level control.<sup>[2b-d,i-k]</sup> To date, two main strategies have been adopted to advance the field of molecular CO<sub>2</sub>RR catalysis: (1) primary coordination sphere chemistry with ligand modifications to tune redox properties of metal centers,<sup>[3]</sup> and (2) secondary coordination sphere chemistry to introduce functionalities beyond the primary active site, including charged<sup>[4]</sup> or hydrogen-bonding groups,<sup>[4h,5]</sup> to promote capture and transformation of CO<sub>2</sub> and its reduced intermediates. For the latter strategy, we have initiated a program to explore a supramolecular second-sphere approach to enhance CO<sub>2</sub>RR<sup>[6]</sup> and related small-molecule activation reactions<sup>[7]</sup> by integrating planar molecular catalysts into three-dimensional confined space architectures. In particular, porous molecular cages, such as metal-organic coordination cages (MOCs)<sup>[8]</sup> and porous organic cages (POCs),<sup>[9]</sup> offer the ability to organize reaction substrates<sup>[10]</sup> and intermediates,<sup>[11]</sup> as well as tune reaction kinetics,<sup>[12]</sup> thus capturing the functional essence of enzyme-substrate binding processes.<sup>[13]</sup> As discrete molecular analogs of extended covalent organic framework (COF)<sup>[14]</sup> and metal organic framework (MOF)<sup>[15]</sup> materials used for CO<sub>2</sub>RR, porous molecular cages offer comparable advantages of permanent porosity in confined spaces with higher solution processibility and homogeneous molecular control.<sup>[16]</sup>

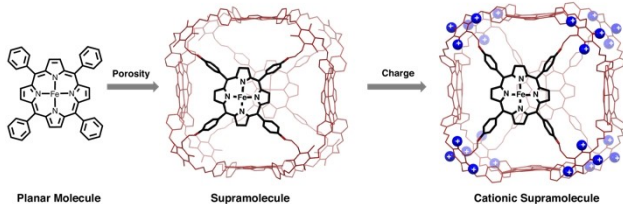
However, despite early advances in the development of molecular cages for energy conversion reactions, these structures largely utilize only one second-sphere feature to augment catalysis—porosity. As such, we sought to incorporate additional second-sphere functionalities into such scaffolds, reasoning that synergy between multiple types of interactions could achieve higher cooperative gains in activity and/or selectivity compared to a single type of interaction. We now report the design, synthesis, and evaluation of a modular porphyrin-based organic cage platform that incorporates dual features of porosity and charge; these multiple second-sphere effects coordinate to amplify photochemical CO<sub>2</sub>RR catalysis beyond incorporation of individual second-sphere elements alone (Scheme 1). An alkyne-functionalized iron porphyrin box (**FePB-1(A)**) synthon enables addition of 24 positively-charged ammonium groups via click chemistry to afford **FePB-2(P)**. CO<sub>2</sub>RR activity comparisons across a systematic series of analogs that feature only porosity (**FePB-3(N)**) or charge (**Fe-p-TMA**) reveal that the dual-functionalized **FePB-2(P)** catalyst enhances CO<sub>2</sub>RR catalysis by over 40-fold over the parent **FeTPP** compound. In contrast, porosity-only or

[\*] Dr. L. An,<sup>+</sup> P. De La Torre,<sup>\*</sup> Dr. P. T. Smith, Dr. M. R. Narouz, Prof. C. J. Chang  
Department of Chemistry, University of California, Berkeley  
94720-1460 Berkeley, CA (USA)  
and  
Chemical Sciences Division, Lawrence Berkeley National Laboratory  
94720-1460 Berkeley, CA (USA)  
E-mail: chrischang@berkeley.edu

Prof. C. J. Chang  
Department of Molecular and Cell Biology, University of California, Berkeley  
94720-1460 Berkeley, CA (USA)

[+] These authors contributed equally to this work.

[\*\*] A previous version of this manuscript has been deposited on a preprint server (<https://doi.org/10.26434/chemrxiv-2022-c4sbr>).



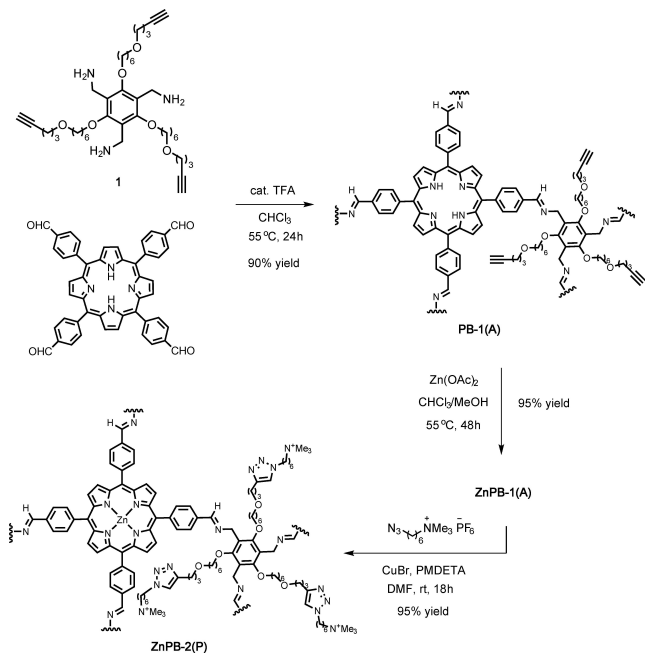
**Scheme 1.** The design of supramolecular  $\text{CO}_2$  reduction reaction ( $\text{CO}_2\text{RR}$ ) catalysts based on iron porphyrin organic cages that incorporate cooperative second-sphere porosity and charge effects.

charge-only interactions give more modest 4-fold or 6-fold increases, respectively. **FePB-2(P)** promotes efficient  $\text{CO}_2\text{RR}$  with 97 % selectivity for CO product, achieving TON exceeding 1100 and initial  $\text{TOF}_{\text{max}}$  reaching 160 min<sup>-1</sup> per Fe center. These results provide a starting point for the broader incorporation of multiple, synergistic second-sphere functionalities as a design element to enhance catalysis in confined molecular spaces.

## Results and Discussion

### Synthesis and Characterization of a Modular Porous Porphyrin Cage Platform Bearing Peripheral Positive Charges

To start, motivated by broader interest in the development of methods for modular post-synthetic modifications of molecular cages,<sup>[17]</sup> we designed and prepared the alkyne-containing clickable porphyrin box **PB-1(A)** starting from an alkyne functionalized triamine linker **1** (Scheme S1). The reported procedure for the unfunctionalized **PB** linker 1,3,5-tris(aminomethyl)-2,4,6-trialkylbenzene features a bromomethylation/azidation/reduction sequence to introduce the three aminomethyl groups.<sup>[18]</sup> However, the harsh conditions required in the bromomethylation step (HOAc/HBr, 70 °C, 18 h) prevented us from introducing the alkynyl functionality in the early stage of the synthesis. Instead, three 1-chloro-hexyl groups were selectively introduced by substitution of phloroglucinol and 1-bromo-6-chlorohexane, which were well tolerated in the bromomethylation step and provided accessible chloric handles for late-stage alkynylation. The chloride groups were successfully converted to terminal aldehyde groups by a bromination/hydrolysis/oxidation sequence. However, neither the Seyerth–Gilbert homologation nor the Corey–Fuchs reaction was successful in transforming these aldehydes into terminal alkyne functionalities.<sup>[19]</sup> After screening several reaction conditions, the alkynyl groups were introduced via an iron-catalyzed reductive etherification reaction of carbonyl with triethylsilane and trimethyl(pent-4-yn-1-yloxy)silane in 93 % yield.<sup>[20]</sup> Upon deprotection with hydrazine, alkyl functionalized triamine linker (**1**) was obtained. The alkyne functionalized **PB-1(A)** was then assembled in 90 % yield by condensing eight triamine linkers (**1**) and six tetraformyl-phenylporphyrin building blocks in  $\text{CHCl}_3$  solution with a catalytic amount of TFA (Scheme 2).<sup>[18]</sup> **PB-1(A)** was



**Scheme 2.** Synthesis of the alkyne-functionalized porphyrin cage **PB-1(A)** and the Zn-metallated, charged porphyrin cage **ZnPb-2(P)**.

thoroughly characterized by NMR, FT-IR, and UV/Vis spectroscopies as well as MALDI mass spectrometry and elemental analysis; the presence of 24 terminal alkynes was confirmed by the observation of a triplet at 1.94 ppm in the <sup>1</sup>H NMR spectrum (Figure S13) and a sharp peak at 3293 cm<sup>-1</sup> corresponding to the C–H stretch of the terminal alkynes detected by FT-IR (Figure S17). Notably, this **PB-1(A)** cage serves as a versatile synthon for further functionalization by copper-catalyzed azide-alkyne cycloaddition (CuAAC) click chemistry, after its metalation with zinc acetate to prevent copper insertion into the porphyrin during the click reaction. Initial pilot screening reactions between **ZnPb-1(A)** and  $\text{N}_3^-(\text{CH}_2)_6\text{NMe}_3^+\text{PF}_6^-$  using typical conditions:<sup>[21]</sup>  $\text{CuSO}_4$  (1.0 equiv, 4.2 mol % per alkyne) and sodium ascorbate (2.0 equiv, 8.4 mol % per alkyne) in a *t*BuOH/H<sub>2</sub>O solvent mixture at room temperature resulted in no product isolated after 24 hours (Table S1, entry 1). Further optimization attempts involving changes in catalyst loading, solvent, and reaction temperature failed to yield the desired product (Table S1, Entries 2–4). To simplify the reaction system, we turned to Cu<sup>1</sup> as a catalyst in anhydrous DMF solution. Unfortunately, neither catalytic nor stoichiometric quantities of CuI or Cu(PPh<sub>3</sub>)<sub>3</sub>Br were successful, even after raising the temperature to 60 °C (Table S1, Entries 5–8). Finally, we were able to obtain the desired product using click-type polymerization conditions<sup>[22]</sup> consisting of CuBr (24.0 equiv) with pentamethyl-diethylenetriamine (PMDETA) (24.0 equiv). The positively charged **ZnPb-2(P)** organic cage was prepared in 95 % isolated yield as confirmed by <sup>1</sup>H- and <sup>19</sup>F NMR, UV/Vis, FT-IR, and elemental analysis (Scheme 2). <sup>1</sup>H NMR analysis of **ZnPb-2(P)** in CD<sub>3</sub>CN showed a new peak at 6.70 ppm with an integral of 24 protons (Figure S24), which

was assigned as the triazole signal. Moreover, the singlet at 2.68 ppm corresponding to the trimethylammonium group and the multiple at 0.60–1.70 ppm assigned to alkyl chains further demonstrated the successful addition of  $\text{N}_3-(\text{CH}_2)_6-\text{NMe}_3^+$  to **ZnPB-1(A)**. The presence of  $\text{PF}_6^-$  counter anions was confirmed by observation of a doublet at  $-72.6$  ppm by  $^{19}\text{F}$  NMR (Figure S25). Elemental analysis revealed a nitrogen percentage increase from 6.66 % (6.72 % calculated) to 10.89 % (11.25 % calculated) as a consequence of the formed triazole rings and added quaternary ammonium groups, while carbon percentage decreased from 74.53 % (74.91 % calculated) to 53.90 % (56.27 % calculated). Moreover, we were able to characterize **ZnPB-2(P)** using electrospray ionization mass spectrometry (ESI-MS). The multiply charged ions distribution from +13 to +20 were observed as **ZnPB-2(P)** losing the corresponding number of counterions ( $\text{PF}_6^-$ ) ions (Table S2, Figures S28–S36). Taken together, these data further confirm successful **PB** modification through a modular post-synthetic click chemistry method.

#### Synthesis, Redox Behavior, and Electrochemical $\text{CO}_2$ Reduction Activity of Porous Iron Porphyrin Cage Analogs With or Without Additional Charged Functionalities

To systematically evaluate the effects of second-sphere porosity and charge within these confined space  $\text{CO}_2$ RR catalysts, we synthesized the Fe analogs of the alkyne-functionalized, neutral, and highly positively charged porphyrin boxes, **FePB-1(A)**, **FePB-3(N)**, and **FePB-2(P)**, respectively (Figure 1a). It is noteworthy that the charged **FePB-2(P)** organic cage is soluble in both DMF and  $\text{CH}_3\text{CN}$  solvents at up to 1 mM concentrations, which is uncommon in **PB** supramolecules.<sup>[23]</sup> The newly-synthesized **FePB** cages, as well as the mononuclear **FeTPP** and the tetracationic **Fe-p-TMA**, which provide control compounds for electrostatic effects in planar mononuclear catalysts, were first compared by cyclic voltammetry (CV) using a glassy carbon electrode. The CV of **FePB-1(A)** under an Ar atmosphere shows three redox waves at  $E_{1/2} = -0.62$ ,  $-1.52$ , and  $-2.11$  V vs. ferrocene/ferrocenium ( $\text{Fc}/\text{Fc}^+$ ), which we assigned as the formal  $\text{Fe}^{\text{III}}/\text{Fe}^{\text{II}}$ ,  $\text{Fe}^{\text{II}}/\text{Fe}^{\text{I}}$ , and  $\text{Fe}^{\text{I}}/\text{Fe}^{\text{0}}$  redox couples, respectively (Figure 1b). The slight positive shift of  $\text{Fe}^{\text{I}}/\text{Fe}^{\text{0}}$  couple in **FePB-1(A)** compared to **FeTPP** ( $E_{1/2} = -2.15$  V) is likely the result of the electron-withdrawing effect of the imine linkages in the porphyrin box. However, these data show that supramolecular encapsulation has modest effects on intrinsic redox properties of molecular porphyrin building blocks. **FePB-3(N)** displays a similar  $\text{Fe}^{\text{I}}/\text{Fe}^{\text{0}}$  couple ( $E_{1/2} = -2.10$  V) to **FePB-1(A)**, indicating the triazole formed after the click reaction also has little effect on the redox potential of the iron centers, while the broadening of the  $\text{Fe}^{\text{III}}/\text{Fe}^{\text{II}}$  and  $\text{Fe}^{\text{II}}/\text{Fe}^{\text{I}}$  redox couples may be due to increased molecular complexity or varied metal ligation by solvent or counter-anion. Interestingly, a 150-mV positive shift of the  $\text{Fe}^{\text{I}}/\text{Fe}^{\text{0}}$  wave was observed in **FePB-2(P)** ( $E_{1/2} = -1.95$  V) compared with **FePB-1(A)** (Figure 1b). The electrostatic effect of introducing twenty-four trimethylammonium groups onto

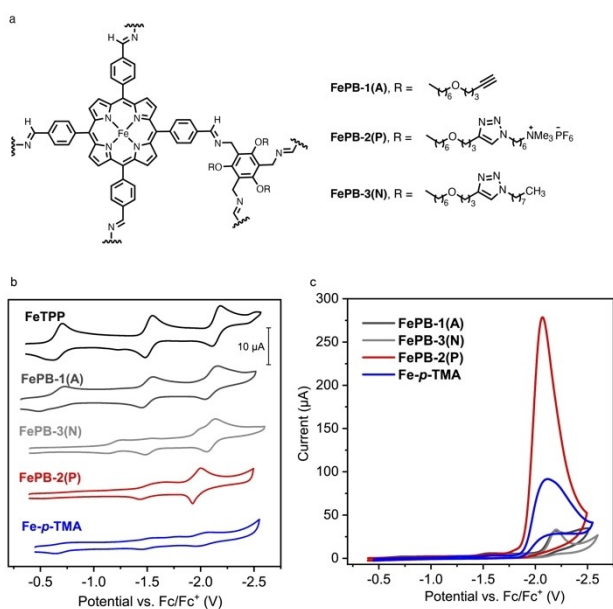


**Figure 1.** a) Structures of the alkyne porous cage synthon **FePB-1(A)**, the neutral porous cage **FePB-3(N)**, and the charged porous cage **FePB-2(P)**. Electrochemical characterization in 0.1 M  $\text{Bu}_4\text{NPF}_6$ /DMF of 0.1 mM **FePB-1(A)** (dark grey), **-2(P)** (red), **-3(N)** (light grey), 0.6 mM **FeTPP** (black) and **Fe-p-TMA** (blue) under b) Argon atmosphere and c)  $\text{CO}_2$  atmosphere with 1 M TFE as a proton source.

the periphery of a porous porphyrin cage scaffold is similar to what was reported for the inductive effect of adding four trimethylanilinium groups to a planar **FeTPP** compound in **Fe-p-TMA** ( $E_{1/2} = -2.00$  V).<sup>[24]</sup> This charge effect is also responsible for a significant shift of  $E_{\text{cat0}}$  toward positive potentials (see below). Upon the addition of  $\text{CO}_2$  and 1.0 M 2,2,2-trifluoroethanol (TFE) as a proton source, a large current increase is observed for **FePB-2(P)**, indicating fast  $\text{CO}_2$  reduction catalysis (Figure 1c). The peak catalytic current under  $\text{CO}_2$  for **FePB-2(P)** is substantially higher than that for each of the non-porous or non-cationic catalysts studied. In order to quantify product selectivity and evaluate the electrochemical stability of **FePB-2(P)**, controlled potential electrolysis (CPE) experiments at various applied potentials were conducted in  $\text{CO}_2$ -saturated acetonitrile solutions with 1.0 M TFE as the proton source and 1.67  $\mu\text{M}$  of catalyst (10  $\mu\text{M}$  Fe). Carbon monoxide (CO) was detected as the major product with a Faradaic efficiency (FE) of ca. 80 %. The low catalyst loading demonstrated the high activity of **FePB-2(P)** for electrochemical  $\text{CO}_2$ RR, which gave a high total TON of 2656 within one hour (Figure S53).

#### Photochemical $\text{CO}_2$ Reduction Activity of Porous Iron Porphyrin Cage Analogs With or Without Additional Charged Functionalities

Encouraged that **FePB-2(P)** is capable of electrochemical  $\text{CO}_2$ RR activity, we turned our attention to light-driven  $\text{CO}_2$  reduction catalysis. In a typical experiment, 2  $\mu\text{M}$  **FePB-**

**2(P)** catalyst was added to a CO<sub>2</sub>-saturated CH<sub>3</sub>CN solution containing 200 μM Tris[2-phenylpyridinato-C<sup>2,N</sup>]iridium (III) (Ir(ppy)<sub>3</sub>) as a photosensitizer, 100 mM 1,3-dimethyl-2-phenyl-2,3-dihydro-1H-benz[d]imidazole (BIH) as a sacrificial electron donor, and 1 M TFE as a proton source; the

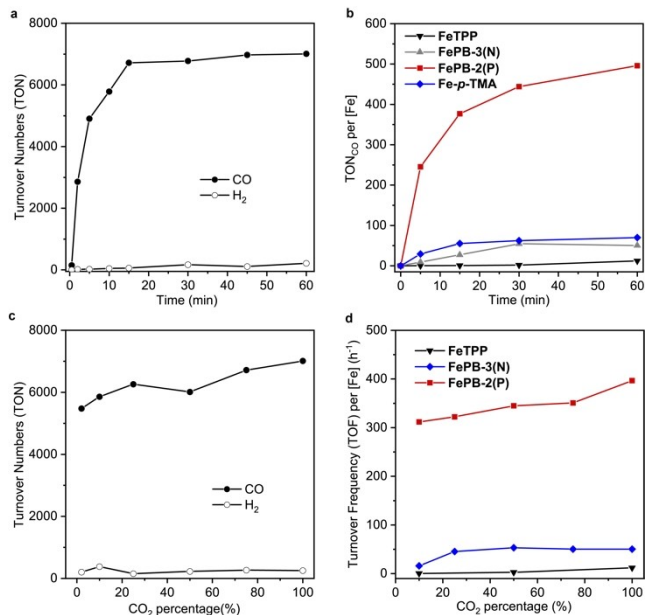


**Figure 2.** a) Photocatalytic CO<sub>2</sub>RR activity of **FePB-2(P)** in CO<sub>2</sub>-saturated CH<sub>3</sub>CN. b) Photocatalytic CO<sub>2</sub>RR activity of **FePB-2(P)** in CO<sub>2</sub>-saturated DMF, comparing TON per [Fe] to **FePB-3(N)**, **FeTPP**, and **Fe-p-TMA**. c) Photochemical CO<sub>2</sub>RR reduction activity of **FePB-2(P)** in CH<sub>3</sub>CN under varying CO<sub>2</sub> concentrations, showing activity down to 2% CO<sub>2</sub>. d) Photochemical CO<sub>2</sub>RR activity of **FePB-2(P)** in DMF under varying CO<sub>2</sub> concentrations, showing a comparison per [Fe] between **FePB-2(P)**, **FePB-3(N)**, and **FeTPP**. **FePB-2(P)** is active down to 5% CO<sub>2</sub> concentrations. Conditions: 2 μM **FePB** or 12 μM mononuclear catalyst, 200 μM Ir(ppy)<sub>3</sub>, 100 mM BIH, and 1 M TFE.

**Table 1:** Photocatalytic activity of [Fe] under various conditions.

Entry	Catalyst	TON Per [Fe] CO	TON Per [Fe] H <sub>2</sub>	TOF <sub>[Fe]</sub> <sup>max</sup> [min <sup>-1</sup> ] <sup>[h]</sup>	Selectivity CO [%]
1 <sup>[a]</sup>	<b>FePB-2(P)</b>	1168	42	164	97
2	<b>FePB-2(P)</b>	496	7	49	98
3	<b>FePB-3(N)</b>	50	7	1.9	88
4	<b>FeTPP</b>	12	5	0.08	70
5	<b>Fe-p-TMA</b>	70	10	5.8	88
6 <sup>[b]</sup>	None	0	1	—	—
7 <sup>[c]</sup>	<b>FePB-2(P)</b>	0	182	—	—
8 <sup>[d]</sup>	<b>FePB-2(P)</b>	40	143	—	22
9 <sup>[e]</sup>	<b>FePB-2(P)</b>	0	0	—	—
10 <sup>[f]</sup>	<b>FePB-2(P)</b>	0	0	—	—
11 <sup>[g]</sup>	<b>FePB-2(P)</b>	33	0	—	100

Reaction Conditions: 200 μM Ir(ppy)<sub>3</sub>, 100 mM BIH, 1 M TFE after 1 hour irradiation in a CO<sub>2</sub> saturated DMF solution unless otherwise noted; control experiment data collected after 30-minute irradiation in entries 6–11. [a] In CH<sub>3</sub>CN. [b] Without **FePB-2(P)** catalyst. [c] Under Ar atmosphere. [d] Without TFE. [e] Without BIH. [f] Without light irradiation. [g] Without Ir(ppy)<sub>3</sub>. [h] Within the first 5 minutes of the reaction, per [Fe].

reactions were irradiated using a 440 nm blue LED light source. Figure 2a shows the catalytic activity of **FePB-2(P)** over a 1-hour period. Within the first two minutes of the reaction, a TOF<sub>max</sub> of 1429 min<sup>-1</sup> is reached; rates of this magnitude are unprecedented for homogeneous Fe porphyrin photocatalysts.<sup>[25]</sup> After a 1-hour photolysis period, we obtained a TON of 7006 per box (1168 per Fe center) with 97 % selectivity for CO. Control experiments performed show that the catalyst, CO<sub>2</sub>, proton source, sacrificial electron donor, light, and photosensitizer, are all required for activity (Table 1, Entries 6–11). Stern–Volmer analysis of the Ir(ppy)<sub>3</sub> excited state was used in order to determine a photocatalytic mechanism. We measured a bimolecular quenching rate constant ( $k_q$ ) of  $1.79 \times 10^{11} \text{ M}^{-1} \text{ s}^{-1}$  in CH<sub>3</sub>CN between Ir(ppy)<sub>3</sub> and **FePB-2(P)** with no emission quenching observed using BIH (Figure S54), indicative of an oxidative quenching mechanism. All other catalysts gave similar quenching rate constants when measured in DMF (Figure S55). The quantum yield for CO production was determined to be  $\Phi = 5.75\%$  by ferrioxalate actinometry (see Supporting Information for details).

To disentangle contributions of second-sphere porosity and charge in **FePB-2(P)**, we evaluated the photocatalytic activity of **FeTPP**, **Fe-p-TMA**, and **FePB-3(N)**. To achieve a fair comparison and to ensure homogeneous conditions for all the catalysts, we used DMF as the solvent, increased catalyst concentration to 12 μM for mononuclear Fe porphyrins and corrected turnover number per iron center (TON<sub>[Fe]</sub>) to reflect activity per Fe center, assuming there are 6 active iron centers per molecule of **FePB** catalyst. Figure 2b shows the photocatalytic activity of **FeTPP**, **Fe-p-TMA**, **FePB-3(N)**, and **FePB-2(P)** after 1-hour irradiation in CO<sub>2</sub>-saturated DMF using the same standard conditions. We observe that the neutral porous cage catalyst **FePB-3(N)** outperforms **FeTPP**, which we attribute to enhanced substrate confinement effects in porous catalyst structures,<sup>[6]</sup> giving **FePB-3(N)** a 4-fold higher TON<sub>[Fe]</sub> and superior CO selectivity of 88 % (Figure 2b). The previously reported<sup>[25b,c]</sup> incorporation of four trimethylanilinium groups into an **FeTPP** framework is reproduced under these conditions, showing higher selectivity and 6-fold higher TON value for CO<sub>2</sub>RR with **Fe-p-TMA** (FE<sub>CO</sub> = 88 %, TON<sub>[Fe]</sub> = 70) compared to **FeTPP** (FE<sub>CO</sub> = 70 %, TON<sub>[Fe]</sub> = 12).

Interestingly, the data reveal that **FePB-2(P)**, which is endowed with both electrostatic and porosity functionalities, achieves a TON<sub>[Fe]</sub> of 496 after 1 h irradiation, representing a 41-fold increase in CO<sub>2</sub>RR activity over the parent **FeTPP** catalyst. This enhancement is larger than what is observed for porosity-only **FePB-(N)** (4-fold) and charge-only **Fe-p-TMA** (6-fold) congeners, suggesting that integrating dual porosity and electrostatic interactions onto a single platform can work together to enhance photocatalytic CO<sub>2</sub>RR activity in synergistic manner (Figure 2b, Table 1, Entries 1–5). Moreover, the high activity of **FePB-2(P)** enables photochemical CO<sub>2</sub>RR to proceed under low CO<sub>2</sub> concentrations.<sup>[26]</sup> Indeed, Figure 2c shows **FePB-2(P)** achieves a CO TON of 5476 with as little as 2% CO<sub>2</sub> in CH<sub>3</sub>CN, maintaining 78 % of its activity compared to saturated CO<sub>2</sub> conditions. We speculate that the ability of

**FePB-2(P)** to maintain high relative CO<sub>2</sub>RR rates even at low CO<sub>2</sub> concentrations may be attributed to the propensity of the porous organic cage to promote both carbon capture and conversion.<sup>[6,18]</sup> We then compared the CO<sub>2</sub>RR activity per [Fe] of **FePB-2(P)** with **FeTPP** and **FePB-3(N)** in DMF (Figure 2d). Going from the planar **FeTPP** catalyst to three-dimensional porous **FePB-3(N)** cage results in an 18-fold increase in TOF under 50 % CO<sub>2</sub> concentrations, suggesting that porosity can play a critical role in facilitating substrate capture and conversion. Moreover, combining second-sphere porosity and charge in **FePB-2(P)** further augments the system, resulting in a 15-fold increase in TOF compared to **FePB-3(N)** at 2 % CO<sub>2</sub> levels.

## Conclusion

To close, we have presented a supramolecular approach to enhancing photochemical CO<sub>2</sub>RR in confined spaces through synergistic second-sphere porosity and charge effects. We enabled this strategy through the modular post-synthetic modification of porous porphyrin organic cages, where the incorporation of 24 alkyne groups provides a versatile platform for further functionalization via click chemistry. Using this synthon, addition of neutral carbon chain and cationic trimethylammonium groups onto the periphery of the cage scaffold affords **FePB-3(N)** and **FePB-2(P)** supramolecules featuring porosity-only and dual porosity/charge effects, respectively. Comparison of these catalysts with a planar **Fe-p-TMA** catalyst with charge-only effects establishes that dual second-sphere porosity and charge interactions can augment CO<sub>2</sub>RR activity in a cooperative manner, exceeding the additive performance of introducing porosity or charge alone. **FePB-2(P)** achieves efficient CO<sub>2</sub>RR with 97 % selectivity for CO, TON of 7006, and initial TOF rate of 1429 min<sup>-1</sup>. Moreover, these combined effects enable retention of efficient photochemical CO<sub>2</sub>RR activity at concentrations of CO<sub>2</sub> down to 2 %. This work highlights the use of multiple synergistic second-sphere interactions as an effective design strategy to enhance CO<sub>2</sub> capture and conversion activity, a concept that can be applied to a broader array of small-molecule activation reactions.

## Acknowledgements

This work was supported by the U.S. Department of Energy, Office of Science, Office of Advanced Scientific Computing, Office of Basic Energy Sciences, via the Division of Chemical Sciences, Geosciences, and Bioscience of the U.S. Department of Energy at Lawrence Berkeley National Laboratory (Grant No. DE-AC02-05CH11231 to C.J.C.). We thank UC Berkeley's NMR facility in the College of Chemistry (CoC NMR) for spectroscopic assistance. Instruments in the CoC NMR are supported in part by NIH (S10OD024998). L.A. thanks SIOC/Pharmaron for a postdoctoral fellowship. P.D. and P.T.S. acknowledge the NSF for a Graduate Research Fellowship. M.R.N. thanks

NSERC for a postdoctoral fellowship. C.J.C. is a CIFAR Fellow.

## Conflict of Interest

The authors declare no conflict of interest.

## Data Availability Statement

The data that support the findings of this study are available in the Supporting Information of this article.

**Keywords:** Carbon Dioxide Reduction · Electrocatalysis · Photocatalysis · Porous Cage · Second-Sphere

- [1] a) N. S. Lewis, D. G. Nocera, *Proc. Natl. Acad. Sci. USA* **2006**, *103*, 15729–15735; b) P. De Luna, C. Hahn, D. Higgins, S. A. Jaffer, T. F. Jaramillo, E. H. Sargent, *Science* **2019**, *364*, eaav3506; c) A. H. Proppe, Y. C. Li, A. Aspuru-Guzik, C. P. Berlinguette, C. J. Chang, R. Cogdell, A. G. Doyle, J. Flick, N. M. Gabor, R. van Grondelle, S. Hammes-Schiffer, S. A. Jaffer, S. O. Kelley, M. Leclerc, K. Leo, T. E. Mallouk, P. Narang, G. S. Schlau-Cohen, G. D. Scholes, A. Vojvodic, V. W.-W. Yam, J. Y. Yang, E. H. Sargent, *Nat. Rev. Mater.* **2020**, *5*, 828–846; d) A. M. Appel, J. E. Bercaw, A. B. Bocarsly, H. Dobbek, D. L. DuBois, M. Dupuis, J. G. Ferry, E. Fujita, R. Hille, P. J. A. Kenis, C. A. Kerfeld, R. H. Morris, C. H. F. Peden, A. R. Portis, S. W. Ragsdale, T. B. Rauchfuss, J. N. H. Reek, L. C. Seefeldt, R. K. Thauer, G. L. Waldrop, *Chem. Rev.* **2013**, *113*, 6621–6658.
- [2] a) Y. Hori in *Modern Aspects of Electrochemistry* (Eds.: C. G. Vayenas, R. E. White, M. E. Gamboa-Aldeco), Springer New York, New York, **2008**, pp. 89–189; b) E. E. Benson, C. P. Kubicki, A. J. Sathrum, J. M. Smieja, *Chem. Soc. Rev.* **2009**, *38*, 89–99; c) C. Costentin, M. Robert, J.-M. Savéant, *Chem. Soc. Rev.* **2013**, *42*, 2423–2436; d) R. Francke, B. Schille, M. Roemelt, *Chem. Rev.* **2018**, *118*, 4631–4701; e) S. Nitopi, E. Bertheussen, S. B. Scott, X. Liu, A. K. Engstfeld, S. Horch, B. Seger, I. E. L. Stephens, K. Chan, C. Hahn, J. K. Nørskov, T. F. Jaramillo, I. Chorkendorff, *Chem. Rev.* **2019**, *119*, 7610–7672; f) S. Zhang, Q. Fan, R. Xia, T. J. Meyer, *Acc. Chem. Res.* **2020**, *53*, 255–264; g) P. T. Smith, E. M. Nichols, Z. Cao, C. J. Chang, *Acc. Chem. Res.* **2020**, *53*, 575–587; h) P. Saha, S. Amanullah, A. Dey, *Acc. Chem. Res.* **2022**, *55*, 134–144; i) E. Boutin, L. Merakeb, B. Ma, B. Boudy, M. Wang, J. Bonin, E. Anxolabéhère-Mallart, M. Robert, *Chem. Soc. Rev.* **2020**, *49*, 5772–5809; j) A. Wagner, C. D. Sahm, E. Reisner, *Nat. Catal.* **2020**, *3*, 775–786; k) A. W. Nichols, C. W. Machan, *Front. Chem.* **2019**, *7*, 397; l) H. S. Shafaat, J. Y. Yang, *Nat. Catal.* **2021**, *4*, 928–933.
- [3] a) I. Azcarate, C. Costentin, M. Robert, J.-M. Savéant, *J. Phys. Chem. C* **2016**, *120*, 28951–28960; b) B. A. Johnson, S. Maji, H. Agarwala, T. A. White, E. Mijangos, S. Ott, *Angew. Chem. Int. Ed.* **2016**, *55*, 1825–1829; *Angew. Chem.* **2016**, *128*, 1857–1861; c) S. Gonell, J. Lloret-Fillol, A. J. M. Miller, *ACS Catal.* **2021**, *11*, 615–626; d) K. Kosugi, M. Kondo, S. Masaoka, *Angew. Chem. Int. Ed.* **2021**, *60*, 22070–22074; *Angew. Chem.* **2021**, *133*, 22241–22245; e) W. Nie, D. E. Tarnopol, C. C. L. McCrory, *J. Am. Chem. Soc.* **2021**, *143*, 3764–3778; f) J. S. Derrick, M. Loipersberger, R. Chatterjee, D. A. Iovan, P. T. Smith, K. Chakarawet, J. Yano, J. R. Long, M. Head-Gordon, C. J.

- Chang, *J. Am. Chem. Soc.* **2020**, *142*, 20489–20501; g) P. De La Torre, J. S. Derrick, A. Snider, P. T. Smith, M. Loipersberger, M. Head-Gordon, C. J. Chang, *ACS Catal.* **2022**, *12*, 8484–8493.
- [4] a) I. Azcarate, C. Costentin, M. Robert, J.-M. Savéant, *J. Am. Chem. Soc.* **2016**, *138*, 16639–16644; b) R. Zhang, J. J. Warren, *J. Am. Chem. Soc.* **2020**, *142*, 13426–13434; c) J. D. Erickson, A. Z. Preston, J. C. Linehan, E. S. Wiedner, *ACS Catal.* **2020**, *10*, 7419–7423; d) J. M. Barlow, J. W. Ziller, J. Y. Yang, *ACS Catal.* **2021**, *11*, 8155–8164; e) D. J. Martin, J. M. Mayer, *J. Am. Chem. Soc.* **2021**, *143*, 11423–11434; f) Y. Mao, M. Loipersberger, K. J. Kron, J. S. Derrick, C. J. Chang, S. M. Sharada, M. Head-Gordon, *Chem. Sci.* **2021**, *12*, 1398–1414; g) S. L. Hooe, J. J. Moreno, A. G. Reid, E. N. Cook, C. W. Machan, *Angew. Chem. Int. Ed.* **2022**, *61*, e202109645; *Angew. Chem.* **2022**, *134*, e202109645; h) M. R. Narouz, P. De La Torre, L. An, C. J. Chang, *Angew. Chem. Int. Ed.* **2022**, *61*, e202207666; *Angew. Chem.* **2022**, *134*, e202207666.
- [5] a) M. W. Drover, *Chem. Soc. Rev.* **2022**, *51*, 1861–1880; b) C. Costentin, S. Drouet, M. Robert, J.-M. Savéant, *Science* **2012**, *338*, 90–94; c) C. Costentin, G. Passard, M. Robert, J.-M. Savéant, *Proc. Natl. Acad. Sci. USA* **2014**, *111*, 14990–14994; d) E. Haviv, D. Azaiza-Dabbah, R. Carmieli, L. Avram, J. M. L. Martin, R. Neumann, *J. Am. Chem. Soc.* **2018**, *140*, 12451–12456; e) A. Chapovetsky, M. Welborn, J. M. Luna, R. Haiges, T. F. Miller, S. C. Marinescu, *ACS Cent. Sci.* **2018**, *4*, 397–404; f) S. Sung, X. Li, L. M. Wolf, J. R. Meeder, N. S. Bhuvanesh, K. A. Grice, J. A. Panetier, M. Nippe, *J. Am. Chem. Soc.* **2019**, *141*, 6569–6582; g) P. Gotico, B. Boitrel, R. Guillot, M. Sircoglou, A. Quaranta, Z. Halime, W. Leibl, A. Aukaloo, *Angew. Chem. Int. Ed.* **2019**, *58*, 4504–4509; *Angew. Chem.* **2019**, *131*, 4552–4557; h) P. Gotico, L. Roupnel, R. Guillot, M. Sircoglou, W. Leibl, Z. Halime, A. Aukaloo, *Angew. Chem. Int. Ed.* **2020**, *59*, 22451–22455; *Angew. Chem.* **2020**, *132*, 22637–22641; i) S. Amanullah, P. Saha, A. Dey, *J. Am. Chem. Soc.* **2021**, *143*, 13579–13592; j) E. M. Nichols, J. S. Derrick, S. K. Nistanaki, P. T. Smith, C. J. Chang, *Chem. Sci.* **2018**, *9*, 2952–2960; k) E. M. Nichols, C. J. Chang, *Organometallics* **2019**, *38*, 1213–1218; l) P. T. Smith, S. Weng, C. J. Chang, *Inorg. Chem.* **2020**, *59*, 9270–9278; m) D. Z. Zee, M. Nippe, A. E. King, C. J. Chang, J. R. Long, *Inorg. Chem.* **2020**, *59*, 5206–5217; n) M. Loipersberger, D. Z. Zee, J. A. Panetier, C. J. Chang, J. R. Long, M. Head-Gordon, *Inorg. Chem.* **2020**, *59*, 8146–8160; o) A. W. Nichols, S. L. Hooe, J. S. Kuehner, D. A. Dickie, C. W. Machan, *Inorg. Chem.* **2020**, *59*, 5854–5864; p) J. S. Derrick, M. Loipersberger, S. K. Nistanaki, A. V. Rothweiler, M. Head-Gordon, E. M. Nichols, C. J. Chang, *J. Am. Chem. Soc.* **2022**, *144*, 11656–11663.
- [6] P. T. Smith, B. P. Benke, Z. Cao, Y. Kim, E. M. Nichols, K. Kim, C. J. Chang, *Angew. Chem. Int. Ed.* **2018**, *57*, 9684–9688; *Angew. Chem.* **2018**, *130*, 9832–9836.
- [7] a) M. Gong, Z. Cao, W. Liu, E. M. Nichols, P. T. Smith, J. S. Derrick, Y.-S. Liu, J. Liu, X. Wen, C. J. Chang, *ACS Cent. Sci.* **2017**, *3*, 1032–1040; b) P. T. Smith, Y. Kim, B. P. Benke, K. Kim, C. J. Chang, *Angew. Chem. Int. Ed.* **2020**, *59*, 4902–4907; *Angew. Chem.* **2020**, *132*, 4932–4937; c) P. T. Smith, B. P. Benke, L. An, Y. Kim, K. Kim, C. J. Chang, *ChemElectroChem* **2021**, *8*, 1653–1657.
- [8] a) M. Yoshizawa, J. K. Klosterman, M. Fujita, *Angew. Chem. Int. Ed.* **2009**, *48*, 3418–3438; *Angew. Chem.* **2009**, *121*, 3470–3490; b) D. J. Tranchemontagne, Z. Ni, M. O'Keeffe, O. M. Yaghi, *Angew. Chem. Int. Ed.* **2008**, *47*, 5136–5147; *Angew. Chem.* **2008**, *120*, 5214–5225; c) T. R. Cook, Y.-R. Zheng, P. J. Stang, *Chem. Rev.* **2013**, *113*, 734–777; d) C. J. Brown, F. D. Toste, R. G. Bergman, K. N. Raymond, *Chem. Rev.* **2015**, *115*, 3012–3035; e) E. G. Percástegui, T. K. Ronson, J. R. Nitschke, *Chem. Rev.* **2020**, *120*, 13480–13544; f) C. T. McTernan, J. A. Davies, J. R. Nitschke, *Chem. Rev.* **2022**, *122*, 10393–10437; g) A. J. Gosselin, C. A. Rowland, E. D. Bloch, *Chem. Rev.* **2020**, *120*, 8987–9014; h) C. E. Hauke, T. R. Cook in *Comprehensive Coordination Chemistry III* (Eds.: E. C. Constable, G. Parkin, L. Que, Jr.), Elsevier, Oxford, **2021**, pp. 1074–1085; i) A. J. McConnell, *Chem. Soc. Rev.* **2022**, *51*, 2957–2971.
- [9] a) J. D. Evans, C. J. Sumby, C. J. Doonan, *Chem. Lett.* **2015**, *44*, 582–588; b) P. Ballester, M. Fujita, J. Rebek, *Chem. Soc. Rev.* **2015**, *44*, 392–393; c) G. Zhang, M. Mastalerz, *Chem. Soc. Rev.* **2014**, *43*, 1934–1947; d) S. H. A. M. Leenders, R. Gramage-Doria, B. de Bruin, J. N. H. Reek, *Chem. Soc. Rev.* **2015**, *44*, 433–448; e) T. Hasell, A. I. Cooper, *Nat. Rev. Mater.* **2016**, *1*, 16053; f) A. I. Cooper, *ACS Cent. Sci.* **2017**, *3*, 544–553; g) M. Mastalerz, *Acc. Chem. Res.* **2018**, *51*, 2411–2422; h) R. D. Mukhopadhyay, Y. Kim, J. Koo, K. Kim, *Acc. Chem. Res.* **2018**, *51*, 2730–2738.
- [10] T. A. Bender, R. G. Bergman, K. N. Raymond, F. D. Toste, *J. Am. Chem. Soc.* **2019**, *141*, 11806–11810.
- [11] T. Iwasawa, R. J. Hooley, J. Rebek, *Science* **2007**, *317*, 493–496.
- [12] M. Yoshizawa, M. Tamura, M. Fujita, *Science* **2006**, *312*, 251–254.
- [13] E. Kuah, S. Toh, J. Yee, Q. Ma, Z. Gao, *Chem. Eur. J.* **2016**, *22*, 8404–8430.
- [14] a) S. Lin, C. S. Diercks, Y.-B. Zhang, N. Kornienko, E. M. Nichols, Y. Zhao, A. R. Paris, D. Kim, P. Yang, O. M. Yaghi, C. J. Chang, *Science* **2015**, *349*, 1208–1213; b) C. S. Diercks, S. Lin, N. Kornienko, E. A. Kapustin, E. M. Nichols, C. Zhu, Y. Zhao, C. J. Chang, O. M. Yaghi, *J. Am. Chem. Soc.* **2018**, *140*, 1116–1122; c) S. Yang, W. Hu, X. Zhang, P. He, B. Pattengale, C. Liu, M. Cendejas, I. Hermans, X. Zhang, J. Zhang, J. Huang, *J. Am. Chem. Soc.* **2018**, *140*, 14614–14618; d) Z. Fu, X. Wang, A. M. Gardner, X. Wang, S. Y. Chong, G. Neri, A. J. Cowan, L. Liu, X. Li, A. Vogel, R. Clowes, M. Bilton, L. Chen, R. S. Sprick, A. I. Cooper, *Chem. Sci.* **2020**, *11*, 543–550; e) P. L. Cheung, S. K. Lee, C. P. Kubiak, *Chem. Mater.* **2019**, *31*, 1908–1919; f) N. Huang, K. H. Lee, Y. Yue, X. Xu, S. Irle, Q. Jiang, D. Jiang, *Angew. Chem. Int. Ed.* **2020**, *59*, 16587–16593; *Angew. Chem.* **2020**, *132*, 16730–16736; g) H.-J. Zhu, M. Lu, Y.-R. Wang, S.-J. Yao, M. Zhang, Y.-H. Kan, J. Liu, Y. Chen, S.-L. Li, Y.-Q. Lan, *Nat. Commun.* **2020**, *11*, 497; h) Y.-N. Gong, W. Zhong, Y. Li, Y. Qiu, L. Zheng, J. Jiang, H.-L. Jiang, *J. Am. Chem. Soc.* **2020**, *142*, 16723–16731; i) B. Han, Y. Jin, B. Chen, W. Zhou, B. Yu, C. Wei, H. Wang, K. Wang, Y. Chen, B. Chen, J. Jiang, *Angew. Chem. Int. Ed.* **2022**, *61*, e202114244; *Angew. Chem.* **2022**, *134*, e202114244; j) M. Lu, M. Zhang, J. Liu, Y. Chen, J.-P. Liao, M.-Y. Yang, Y.-P. Cai, S.-L. Li, Y.-Q. Lan, *Angew. Chem. Int. Ed.* **2022**, *61*, e202200003; *Angew. Chem.* **2022**, *134*, e202200003.
- [15] a) N. Kornienko, Y. Zhao, C. S. Kley, C. Zhu, D. Kim, S. Lin, C. J. Chang, O. M. Yaghi, P. Yang, *J. Am. Chem. Soc.* **2015**, *137*, 14129–14135; b) Y.-R. Wang, Q. Huang, C.-T. He, Y. Chen, J. Liu, F.-C. Shen, Y.-Q. Lan, *Nat. Commun.* **2018**, *9*, 4466; c) S. Dou, J. Song, S. Xi, Y. Du, J. Wang, Z.-F. Huang, Z. J. Xu, X. Wang, *Angew. Chem. Int. Ed.* **2019**, *58*, 4041–4045; *Angew. Chem.* **2019**, *131*, 4081–4085; d) N.-Y. Huang, X.-W. Zhang, Y.-Z. Xu, P.-Q. Liao, X.-M. Chen, *Chem. Commun.* **2019**, *55*, 14781–14784; e) X. Kang, B. Wang, K. Hu, K. Lyu, X. Han, B. F. Spencer, M. D. Frogley, F. Tuna, E. J. L. McInnes, R. A. W. Dryfe, B. Han, S. Yang, M. Schröder, *J. Am. Chem. Soc.* **2020**, *142*, 17384–17392; f) H. Zhong, M. Ghorbani-Asl, K. H. Ly, J. Zhang, J. Ge, M. Wang, Z. Liao, D. Makarov, E. Zschech, E. Brunner, I. M. Weidinger, J. Zhang, A. V. Krasheninnikov, S. Kaskel, R. Dong, X. Feng, *Nat. Commun.* **2020**, *11*, 1409; g) X.-F. Qiu, H.-L. Zhu, J.-R. Huang, P.-Q. Liao, X.-M. Chen, *J. Am. Chem. Soc.* **2021**, *143*, 7242–7246; h) H. He, J. A. Perman, G. Zhu, S. Ma, *Small* **2016**, *12*, 6309–6324; i) C. A. Trickett, A. Helal, B. A. Al-Maythalony, Z. H.

- Yamani, K. E. Cordova, O. M. Yaghi, *Nat. Rev. Mater.* **2017**, *2*, 17045; j) M. B. Majewski, A. W. Peters, M. R. Wasielewski, J. T. Hupp, O. K. Farha, *ACS Energy Lett.* **2018**, *3*, 598–611; k) Z. Liang, C. Qu, D. Xia, R. Zou, Q. Xu, *Angew. Chem. Int. Ed.* **2018**, *57*, 9604–9633; *Angew. Chem.* **2018**, *130*, 9750–9780; l) S. S. A. Shah, T. Najam, M. Wen, S.-Q. Zang, A. Waseem, H.-L. Jiang, *Small Struct.* **2022**, *3*, 2100090.
- [16] H. H. Huang, T. Šolomek, *Chimia* **2021**, *75*, 285–290.
- [17] a) H. Wang, Y. Jin, N. Sun, W. Zhang, J. Jiang, *Chem. Soc. Rev.* **2021**, *50*, 8874–8886; b) J. Liu, Z. Wang, P. Cheng, M. J. Zaworotko, Y. Chen, Z. Zhang, *Nat. Chem. Rev.* **2022**, *6*, 339–356.
- [18] S. Hong, M. R. Rohman, J. Jia, Y. Kim, D. Moon, Y. Kim, Y. H. Ko, E. Lee, K. Kim, *Angew. Chem. Int. Ed.* **2015**, *54*, 13241–13244; *Angew. Chem.* **2015**, *127*, 13439–13442.
- [19] a) Z. Wang in *Comprehensive Organic Name Reactions and Reagents* (Ed.: Z. Wang), Wiley, Hoboken, **2010**, pp. 2559–2562; b) Z. Wang in *Comprehensive Organic Name Reactions and Reagents* (Ed.: Z. Wang), Wiley, Hoboken, **2010**, pp. 717–721.
- [20] K. Iwanami, H. Seo, Y. Tobita, T. Oriyama, *Synthesis* **2005**, *2005*, 183–186.
- [21] V. V. Rostovtsev, L. G. Green, V. V. Fokin, K. B. Sharpless, *Angew. Chem. Int. Ed.* **2002**, *41*, 2596–2599; *Angew. Chem.* **2002**, *114*, 2708–2711.
- [22] D. Huang, A. Qin, B. Z. Tang, *Click Polymerization*, The Royal Society of Chemistry, London, **2018**, pp. 36–85.
- [23] B. P. Benke, P. Aich, Y. Kim, K. L. Kim, M. R. Rohman, S. Hong, I.-C. Hwang, E. H. Lee, J. H. Roh, K. Kim, *J. Am. Chem. Soc.* **2017**, *139*, 7432–7435.
- [24] C. Costentin, M. Robert, J.-M. Savéant, A. Tatin, *Proc. Natl. Acad. Sci. USA* **2015**, *112*, 6882–6886.
- [25] a) J. Bonin, M. Robert, M. Routier, *J. Am. Chem. Soc.* **2014**, *136*, 16768–16771; b) H. Rao, L. C. Schmidt, J. Bonin, M. Robert, *Nature* **2017**, *548*, 74–77; c) H. Rao, C.-H. Lim, J. Bonin, G. M. Miyake, M. Robert, *J. Am. Chem. Soc.* **2018**, *140*, 17830–17834; d) E. Pugliese, P. Gotico, I. Wehrung, B. Boitrel, A. Quaranta, M.-H. Ha-Thi, T. Pino, M. Sircoglu, W. Leibl, Z. Halime, A. Aukauloo, *Angew. Chem. Int. Ed.* **2022**, *61*, e202117530; *Angew. Chem.* **2022**, *134*, e202117530; e) X. Zhang, K. Yamauchi, K. Sakai, *ACS Catal.* **2021**, *11*, 10436–10449.
- [26] a) T. Nakajima, Y. Tamaki, K. Ueno, E. Kato, T. Nishikawa, K. Ohkubo, Y. Yamazaki, T. Morimoto, O. Ishitani, *J. Am. Chem. Soc.* **2016**, *138*, 13818–13821; b) H. Kumagai, T. Nishikawa, H. Koizumi, T. Yatsu, G. Sahara, Y. Yamazaki, Y. Tamaki, O. Ishitani, *Chem. Sci.* **2019**, *10*, 1597–1606; c) Y. Yamazaki, M. Miyaji, O. Ishitani, *J. Am. Chem. Soc.* **2022**, *144*, 6640–6660.

Manuscript received: June 27, 2022

Version of record online: December 20, 2022